Solute spreading in nonstationary flows in bounded, heterogeneous unsaturated-saturated media

Zhiming Lu and Dongxiao Zhang

Hydrology, Geochemistry, and Geology Group (EES-6), Los Alamos National Laboratory, Los Alamos, New Mexico, USA

Received 28 August 2001; revised 17 July 2002; accepted 17 July 2002; published 7 March 2003.

[1] It is commonly assumed in stochastic solute (advective) transport models that either the velocity field is stationary (statistically homogeneous) or the mean flow is unidirectional. In this study, using a Lagrangian approach, we develop a general stochastic model for transport in variably saturated flow in randomly heterogeneous porous media. The mean flow in the model is multidirectional, and the velocity field can be nonstationary (with location-dependent statistics). The nonstationarity of the velocity field may be caused by statistical nonhomogeneity of medium properties or complex boundary configurations. The particle's mean position is determined using the mean Lagrangian velocity. Particle spreading (the displacement covariances) is expressed in terms of the state transition matrix that satisfies a time-varying dynamic equation whose coefficient matrix is the derivative of the mean Lagrangian velocity field. In the special cases of stationary velocity fields the transition matrix becomes the identical matrix, and our model reduces to the well-known model of *Dagan* [1984]. For nonstationary but unidirectional flow fields our model reduces to that of *Butera and Tanda* [1999] and *Sun and Zhang* [2000]. The validity of the transport model is examined by comparisons with Monte Carlo simulations for the following three cases: transport in a mean gravity-dominated flow, in an unsaturated flow with a water table boundary, and in a saturated-unsaturated flow. An excellent agreement is found between our model results and those from Monte Carlo simulations. *INDEX TERMS:* 1829 Hydrology: Groundwater hydrology; 1869 Hydrology: Stochastic processes; 1875 Hydrology: Unsaturated zone; 3220 Mathematical Geophysics: Nonlinear dynamics; 3230 Mathematical Geophysics: Numerical solutions; *KEYWORDS:* solute transport, nonstationary flow, heterogeneity, stochastic processes, saturated/unsaturated flow

Citation: Lu, Z., and D. Zhang, Solute spreading in nonstationary flows in bounded, heterogeneous unsaturated-saturated media, *Water Resour. Res.*, *39*(3), 1049, doi:10.1029/2001WR000908, 2003.

1. Introduction

[2] Solute transport in heterogeneous porous media has received great attention in the last three decades. Many stochastic models have been developed for fluid flow and solute transport in the saturated zone [*Gelhar and Axness*, 1983; *Dagan*, 1984, 1989; *Winter et al.*, 1984; *Neuman et al.*, 1987; *Graham and McLaughlin*, 1989; *Rubin*, 1990, 1997; *Shvidler*, 1993; *Cushman and Ginn*, 1993; *Zhang and Neuman*, 1995; *Kavvas and Karakas*, 1996] and in the unsaturated zone [*Dagan and Bresler*, 1979; *Bresler and Dagan*, 1981; *Jury*, 1982; *Jury et al.*, 1986; *Simmons*, 1982; *Polmann et al.*, 1991; *Jury and Scotter*, 1994; *Harter and Yeh*, 1996a, 1996b].

[3] In most of these models it is commonly assumed that medium properties (such as hydraulic conductivity) are spatially stationary, or the mean flow field is uniform and/or unidirectional. *Russo* [1993, 1995a, 1995b, 1998] presented a stochastic macrodispersion model for solute transport in partially saturated, unbounded porous media based on the stochastic flow theory of *Yeh et al.* [1985a, 1985b]. In this model, the mean pressure head is assumed to be constant, and the velocity field is spatially stationary. The flow field considered is thus mean gravity-dominated. For such a case, the displacement covariance expressions are in agreement with those derived by *Dagan* [1984, 1989] for saturated heterogeneous formations. It has been found that in this case, the longitudinal displacement covariance X_{11} increases with travel time, and the rate of increase, reflected as the longitudinal macrodispersion coefficient D_{11}, becomes constant at large time. The transverse displacement covariance X_{22} increases at the early time and approaches constant with time. *Indelman and Rubin* [1996] addressed the problem of solute transport in nonstationary (statistically nonhomogeneous) velocity fields due to a trending conductivity of the porous medium and gave general equations for the first two moments of the particle trajectory with a unidirectional mean velocity. *Butera and Tanda* [1999] derived explicit expressions for particle displacement covariances for solute transport in unidirectional but nonuniform mean flows; *Destouni et al.* [2001] made use of these expressions in studying solute transport under uniform recharge. *Sun and Zhang* [2000] investigated the effect of a water table boundary on solute spreading in an unsaturated porous medium. By first-order approximations they derived statistical moments of particle displacement for the special case of unidirectional but nonuniform mean flow.

One of their results is that near the water table the longitudinal displacement covariance decreases rather than increases linearly at the large time as predicted by previous models.

[4] Recently, *Foussereau et al.* [2001] studied transport of nonreactive solutes through a coupled, two-dimensional randomly heterogeneous unsaturated-saturated zone system with temporally random rainfall using Monte Carlo simulations and compared Monte Carlo simulation results with the theoretical results of *Destouni and Graham* [1995]. In the latter study, although the flow field is nonstationary, the particle displacement covariance was approximated with the modified version of the well-known displacement covariance derived under stationary conditions [*Destouni and Graham*, 1995, equation (18); *Rubin and Bellin*, 1994, equation (17)]. As will be clear later in this paper, this approximation may not be appropriate. In addition, in *Destouni and Graham*'s [1995] model the coupling between the unsaturated and saturated zones is not fully accounted for in that the two flow regimes are solved separately, and the mean flow in the unsaturated zone is set to be vertical while that in the saturated zone is taken to be horizontal.

[5] In this study, we develop a general model to predict the displacement covariance tensor for solute transport in a nonstationary flow field, in which both the mean flow direction and magnitude may vary in space. Flow nonstationarity may be caused by nonstationary medium properties, complex flow configurations, or appropriate boundary conditions (such as a water table boundary) [*Zhang*, 2002]. We express the displacement covariance tensor at any time t in terms of the initial displacement covariance at t_0, Lagrangian velocity covariance, and the state transition matrix, the last of which depends on the derivatives of the mean Lagrangian velocity with respect to the particle path. The first two moments of the particle displacement are then evaluated. The displacement covariances in general have to be evaluated numerically. In the case of uniform, unidirectional mean flow (e.g., mean gravity-dominated flow), our expression reduces to the well-known results of *Dagan* [1984]. Our model is in spirit similar to that of *Indelman and Rubin* [1996]. However, our work differs from the latter in the following two aspects: (1) Indelman and Rubin's main result [*Indelman and Rubin*, 1996, equation (16)] seems to be only valid for weak mean flow nonuniformity while our model does not have this restriction; (2) they only evaluated the special case of unidirectional mean flow while our study looks at transport in coupled unsaturated and saturated flow where the mean flow direction and magnitude may vary significantly in space. In the case of the unidirectional nonstationary flow field, our expression reduces to those of *Butera and Tanda* [1999] and *Sun and Zhang* [2000]. Three examples are given to illustrate the applicability of our model: solute transport in a mean gravity-dominated flow, in an unsaturated flow with a water table boundary, and in a fully coupled unsaturated-saturated flow. Our results are compared with Monte Carlo simulation results and an excellent agreement is found between our model results and those from Monte Carlo simulations. We also compared our results against those obtained using *Dagan*'s [1989] expression for the case of saturated-unsaturated flow. It is shown that the results based on the approach presented in our work are in much better agreement with Monte Carlo simulation results.

2. Mathematical Development

[6] We consider transport of inert solutes in a transient flow in unsaturated-saturated media satisfying the following continuity equation and Darcy's law:

$$\{S_s H(\psi) + H(-\psi) C[\psi, \cdot]\} \frac{\partial \psi(\mathbf{x}, t)}{\partial t} + \nabla \cdot \mathbf{q}(\mathbf{x}, t) = g(\mathbf{x}, t) \quad (1)$$

$$q_i(\mathbf{x}, t) = -K[\psi, \cdot] \frac{\partial}{\partial x_i} [\psi(\mathbf{x}, t) + x_1] \quad (2)$$

subject to initial and boundary conditions

$$\psi(\mathbf{x}, 0) = \Psi_0(\mathbf{x}) \qquad \mathbf{x} \in \Omega \quad (3)$$

$$\psi(\mathbf{x}, t) = \Psi(\mathbf{x}, t), \qquad \mathbf{x} \in \Gamma_D \quad (4)$$

$$\mathbf{q}(\mathbf{X}, t) \cdot \mathbf{n}(\mathbf{x}) = Q(\mathbf{x}, t), \qquad \mathbf{x} \in \Gamma_N \quad (5)$$

where $\mathbf{q}$ is the specific discharge, $\psi + x_1$ is the total head, ψ is the pressure head, $i = 1, \cdots, d$ (where d is the number of space dimensions), $\Psi_0(\mathbf{x})$ is the initial pressure head in the domain Ω, $\Psi(\mathbf{x}, t)$ is the prescribed head-on Dirichlet boundary segments Γ_D, $Q(\mathbf{x}, t)$ is the prescribed flux across Neumann boundary segments Γ_N, $\mathbf{n}(\mathbf{x}) = (n_1, \cdots, n_d)^T$ is an outward unit vector normal to the boundary, $H(\psi)$ is the Heaviside step function, being zero when $\psi < 0$ and one when $\psi \geq 0$, S_s is the specific storage, $C[\psi, \cdot] = d\theta_e/d\psi$ is the specific moisture capacity, $\theta_e \equiv \theta_e[\psi, \cdot]$ is the effective volumetric water content at $\mathbf{x}$, which depends on ψ and soil properties when $\psi < 0$ and becomes the saturated water content θ_s when $\psi \geq 0$, and $K[\psi, \cdot]$ is the unsaturated hydraulic conductivity (assumed to be isotropic locally). Both C and K are functions of pressure head and soil properties at $\mathbf{x}$. The elevation x_1 is directed vertically upward. In these coordinates, recharge has a negative sign. When the flow is unsaturated, it is required to adopt some model to describe the constitutive relationships of K versus ψ and θ_e versus ψ. Although the Brooks-Corey model may have certain mathematical advantages over the Gardner-Russo model [*Gardner*, 1958; *Russo*, 1988] in low-order stochastic analyses [*Zhang et al.*, 1998], we use the latter for simplicity:

$$K(\mathbf{x}, t) = K_s(\mathbf{x}) \exp[\alpha(\mathbf{x}) \psi(\mathbf{x}, t)] \quad (6)$$

$$\theta_e(\mathbf{x}, t) = (\theta_s - \theta_r)\{\exp[0.5\alpha(\mathbf{x})\psi(\mathbf{x}, t)] \cdot [1 - 0.5\alpha(\mathbf{x})\psi(\mathbf{x}, t)]\}^{2/(m+2)} \quad (7)$$

where $\psi \leq 0$. A stochastic model of variably saturated flow on the basis of van Genuchten-Mualem constitutive relationship [*van Genuchten*, 1980] has been developed by *Lu and Zhang* [2002]. In equations (6)–(7), α is the soil parameter related to the pore size distribution, m is a parameter related to tortuosity (taken to be known), θ_r is the residual (irreducible) water content, and θ_s is the saturated water content. The variabilities of θ_s and θ_r are likely to be small compared to that of the effective water content θ_e [*Russo and Bouton*, 1992]. It

is assumed that θ_s, θ_r, and m are deterministic constants while the soil parameter $\alpha(\mathbf{x})$ and the log transformed saturated hydraulic conductivity $f(\mathbf{x}) = \ln K_s(\mathbf{x})$ are treated as random space functions. We also allow spatial variability and/or randomness in the initial and boundary terms $\Psi_0(\mathbf{x})$, $\Psi(\mathbf{x}, t)$, and $Q(\mathbf{x}, t)$, and in the source/sink term $g(\mathbf{x}, t)$. They are generally treated as (spatially and/or temporally) nonstationary random space functions (random fields). Thus the expected values may be space- and time-dependent and the covariances may depend on the actual points in space-time rather than only on their space-time lags.

[7] When the soil properties $f(\mathbf{x})$ and $\alpha(\mathbf{x})$, the initial/boundary conditions $\Psi_0(\mathbf{x})$, $\Psi(\mathbf{x}, t)$, and $Q(\mathbf{x}, t)$, and/or the source/sink terms $g(\mathbf{x}, t)$ are treated as random functions, the governing equations (1)–(5) become a set of stochastic partial differential equations whose solutions are no longer deterministic values but probability distributions or related quantities such as statistical moments of the dependent variables. These equations have been derived analytically and solved numerically by *Zhang and Lu* [2002].

[8] The seepage (Eulerian) velocity at $\mathbf{x}$ is related to the specific flux q_i by

$$u_i(\mathbf{x}, t) = \frac{q_i(\mathbf{x}, t)}{\theta_e(\mathbf{x}, t)}. \tag{8}$$

[9] For a particle originating from location $\mathbf{a}$ at $t = t_0$, its trajectory is described by the following kinetic equation:

$$\frac{d\mathbf{X}(t; \mathbf{a}, t_0)}{dt} = \mathbf{V}[\mathbf{X}(t; \mathbf{a}, t_0)] \tag{9}$$

with the initial condition $\mathbf{X}(t_0; \mathbf{a}, t_0) = \mathbf{a}$, where $\mathbf{X}(t; \mathbf{a}, t_0)$ stands for the particle position at time t and $\mathbf{V}[\mathbf{X}(t; \mathbf{a}, t_0)]$ denotes the (Lagrangian) velocity of the particle. It should be emphasized that even if in the case that the flow field is steady state, the particle (Lagrangian) velocity $\mathbf{V}[\mathbf{X}(t; \mathbf{a}, t_0)]$ may still be time-dependent if the (Eulerian) flow field is spatially nonstationary, which may be caused by, for example, nonstationarity of soil properties or appropriate boundary conditions (such as a water table boundary) [*Zhang*, 2002].

[10] When the Eulerian velocity $u_i(\mathbf{X}, t)$ is treated as a random space function, so should the particle velocity and the particle position. Let us denote $\mathbf{X}(t; \mathbf{a}, t_0)$ as $\mathbf{X}_t$ when there is no confusion. We may decompose the Eulerian velocity $u_i(\mathbf{X}, t)$ and the particle position $\mathbf{X}_t$ into their respective mean and fluctuation: $u_i(\mathbf{X}, t) = \langle u_i(\mathbf{X},t)\rangle + u_i'(\mathbf{X}, t)$, and $\mathbf{X}_t = \langle \mathbf{X}_t\rangle + \mathbf{X}_t'$. With Taylor expansion we may expand the Lagrangian velocity $\mathbf{V}(\mathbf{X}_t)$ at the mean position $\langle \mathbf{X}_t\rangle$ as

$$\mathbf{V}(\mathbf{X}_t) = \mathbf{V}(\langle \mathbf{X}_t\rangle) + (\mathbf{X}_t' \cdot \nabla)\mathbf{V}(\langle \mathbf{X}_t\rangle) + \frac{1}{2}(\mathbf{X}_t' \cdot \nabla)^2\mathbf{V}(\langle \mathbf{X}_t\rangle) + \cdots. \tag{10}$$

Substituting (10) into (9) and collecting terms at zeroth- and first-order leads to

$$\frac{d\langle \mathbf{X}_t\rangle}{dt} = \langle \mathbf{V}(\langle \mathbf{X}_t\rangle)\rangle, \tag{11}$$

$$\frac{d\mathbf{X}_t'}{dt} = \mathbf{V}'(\langle \mathbf{X}_t\rangle) + (\mathbf{X}_t' \cdot \nabla)\langle \mathbf{V}(\langle \mathbf{X}_t\rangle)\rangle \tag{12}$$

with the initial conditions $\langle \mathbf{X}_t\rangle = \mathbf{a}$ and $\mathbf{X}'_t = \mathbf{X}'_0$ at $t = t_0$.

[11] Equation (12) can be rewritten as

$$\frac{dX_{t,i}'}{dt} = V_i'(\langle \mathbf{X}_t\rangle) + B_{ij}(t)X_{t,j}', \tag{13}$$

where $i, j = 1, \cdots, d$, and

$$B_{ij}(t) = \left.\frac{\partial\langle V_i(\mathbf{X}_t)\rangle}{\partial X_{t,j}}\right|_{\mathbf{X}_t = \langle \mathbf{X}_t\rangle}. \tag{14}$$

Summation for repeated indices in (13) is implied. *Indelman and Rubin* [1996] and *Sun and Zhang* [2000] derived (13) and considered some special cases of unidirectional flows on the basis of it. *Indelman and Rubin* [1996] expressed $X_{t,i}'$ in an integral form similar to

$$X_{t,i}' = \int_{t_0}^{t} V_i'(\langle \mathbf{X}_\tau\rangle)d\tau + \int_{t_0}^{t} B_{ij}(\tau)X_{\tau,j}'d\tau. \tag{15}$$

It is seen that the right-hand-side of (15) has the term $X_{\tau,j}'$. Substituting of (15) into its right-hand-side leads to

$$X_{t,i}' = \int_{t_0}^{t} V_i'(\langle \mathbf{X}_\tau\rangle)d\tau + \int_{t_0}^{t}\int_{t_0}^{\tau} B_{ij}(\tau) \cdot \left[V_j'(\langle \mathbf{X}_{\tau'}\rangle) + B_{jl}(\tau')X_{\tau',l}'\right]d\tau' d\tau. \tag{16}$$

Theoretically, (15) or (16) is not closed without an infinite number of substitutions. *Indelman and Rubin* [1996, equation (16)] stopped this process by neglecting the last term in (16) without an explicit justification. It seems that the resulting approximation should be valid when $B_{ij}(t)$ is small. *Sun and Zhang* [2000, equation (10)] were able to represent $X_{\tau,i}'$ of (13) in an exact integral form in terms of an exponential term for the case of unidirectional nonstationary mean flow. It can be shown that the result of *Indelman and Rubin* [1996, equation (16)] is recovered by keeping only the first two terms of the Taylor expansion of the exponential integral in (10) of *Sun and Zhang* [2000]. For the case of $B_{ij}(t) \equiv 0$, (15) reduces to the well-known expression for uniform mean flow [e.g., *Dagan*, 1989].

[12] In this study, we consider the general case of solute spreading in a spatially nonstationary flow field, where the mean flow may vary spatially in both magnitude and direction. For such a general case, explicit analytical expressions for $X_{t,i}'$ are not possible. Hence, we derive the second moments of $X_{t,i}$ on the basis of the general expression (13). Equation (13) can be rewritten in a matrix form as

$$\frac{d\mathbf{X}_t'}{dt} = \mathbf{V}'(\langle \mathbf{X}_t\rangle) + \mathbf{X}\mathbf{B}(t)\mathbf{X}_t' \tag{17}$$

where $\mathbf{X}'_t = (X'_{t,1}, \cdots, X'_{t,d})^T$, $\mathbf{V}' = (V'_1, \cdots, V'_d)^T$, and $\mathbf{B} = (\mathbf{B}_{ij})_{d \times d}$. This equation has a unique solution [Appendix A],

$$\mathbf{X}_t' = \Phi(t, t_0)\mathbf{X}_0' + \int_{t_0}^{t} \Phi(t, \tau)\mathbf{V}'(\langle \mathbf{X}_\tau\rangle)d\tau \tag{18}$$

where $\mathbf{X}'_0 = \mathbf{X}'_{t0}$ is the initial condition for $\mathbf{X}'$, and the $d \times d$ matrix $\Phi(t, t_0)$ is called the state transition matrix

(or fundamental matrix) which satisfies the homogeneous equation

$$\frac{d\Phi(t,t_0)}{dt} = \mathbf{B}(t)\Phi(t,t_0) \tag{19}$$

with initial condition $\Phi(t_0, t_0) = E$, where E is the identity matrix. The solution of (19) can be expressed as the Peano-Baker series [*Antsaklis and Michel*, 1997],

$$\Phi(t,\tau) = E + \int_\tau^t \mathbf{B}(\tau_0)d\tau_0 + \int_\tau^t \mathbf{B}(\tau_0)\int_\tau^{\tau_0} \mathbf{B}(\tau_1)d\tau_1 d\tau_0 + \int_\tau^t \mathbf{B}(\tau_0)\int_\tau^{\tau_0} \mathbf{B}(\tau_1)\int_\tau^{\tau_1} \mathbf{B}(\tau_2)d\tau_2 d\tau_1 d\tau_0 + \cdots. \tag{20}$$

It should be noted that (18) is an exact solution for (17). By retaining the first two terms in the right-hand side of (20), our solution (18) reduced to (16) of *Indelman and Rubin* [1996]. Another advantage of solution (18) is that $\Phi(t, \tau)$ is independent of initial displacement perturbation $\mathbf{X}'_0$ at t_0 and the driving force term $\mathbf{V}'(\langle\mathbf{X}_t\rangle)$; therefore $\Phi(t,\tau)$ calculated for a mean flow field can be used for different displacement perturbation $\mathbf{X}'_0$ and different degree of heterogeneity of the porous medium. This may be useful in model calibration and inverse problems.

[13] Multiplying (18) by itself in terms of t' and using (A3) yields the first-order displacement (cross-) covariance tensor

$$\langle \mathbf{X}'_t \mathbf{X}'^T_{t'} \rangle = \Phi(t,t_0)\langle \mathbf{X}'_0 \mathbf{X}'^T_0 \rangle \Phi^T(t',t_0) + \int_{t_0}^{t'} \Phi(t,t_0)\langle \mathbf{X}'_0 \mathbf{V}'^T(\langle\mathbf{X}_{\tau'}\rangle)\rangle \Phi^T(t',\tau')d\tau' + \int_{t_0}^{t} \Phi(t,\tau)\langle \mathbf{V}'(\langle\mathbf{X}_\tau\rangle)\mathbf{X}'^T_0 \rangle \Phi^T(t',t_0)d\tau + \int_{t_0}^{t}\int_{t_0}^{t'} \Phi(t,\tau)\langle \mathbf{V}'(\langle\mathbf{X}_\tau\rangle)\mathbf{V}'^T(\langle\mathbf{X}_{\tau'}\rangle)\rangle \Phi^T(t',\tau')d\tau' d\tau. \tag{21}$$

It should be pointed out that the cross covariance between the initial displacement and velocity perturbation $\langle \mathbf{X}'_0 \mathbf{V}'^T(\langle\mathbf{X}_\tau\rangle)\rangle$ may not be zero if the particle is released before time t_0. If the displacement perturbation at the initial state $\mathbf{X}'_0 \equiv 0$, for instance at the time of a known release ($t_0 \equiv 0$), (21) simplifies to

$$\langle \mathbf{X}'_t \mathbf{X}'^T_{t'} \rangle = \int_{t_0}^{t}\int_{t_0}^{t'} \Phi(t,\tau)\langle \mathbf{V}'(\langle\mathbf{X}_\tau\rangle)\mathbf{V}'^T(\langle\mathbf{X}_{\tau'}\rangle)\rangle \Phi^T(t',\tau')d\tau' d\tau \tag{22}$$

or in its component form

$$\langle X'_{t,i} X'_{t',j}\rangle = \int_{t_0}^{t}\int_{t_0}^{t'} \Phi_{ik}(t,\tau)\Phi_{jl}(t',\tau')\langle V'_k(\langle\mathbf{X}_\tau\rangle)V'_l(\langle\mathbf{X}_{\tau'}\rangle)\rangle d\tau d\tau'. \tag{23}$$

By setting $t' = t$ in (23) we obtain the displacement (cross-)covariance X_{ij}

$$X_{ij}(t) = \langle X'_{t,i} X'_{t,j}\rangle = \int_{t_0}^{t}\int_{t_0}^{t} \Phi_{ik}(t,\tau)\Phi_{jl}(t,\tau') \cdot \langle V'_k(\langle\mathbf{X}_\tau\rangle)V'_l(\langle\mathbf{X}_{\tau'}\rangle)\rangle d\tau d\tau'. \tag{24}$$

Because $\langle V'_i(\langle\mathbf{X}_\tau\rangle)V'_i(\langle\mathbf{X}_{\tau'}\rangle)\rangle$ is a covariance function for all i, it can be shown mathematically that X_{ii} is a positive quantity for all i. Though $\langle X'_{t,i} X'_{t',j}\rangle$ is asymmetric with respect to indices i and j unless $t \equiv t'$, the tensor $\mathbf{X}$ is symmetric, i.e., $X_{ij}(t) \equiv X_{ji}(t)$ for all i and j.

[14] The dispersion coefficient $D_{ij}(t)$ may be derived by taking the derivative of $X_{ij}(t)$ with respect to t, and noticing that $d\,\Phi_{ij}(t, \tau)/dt = B_{im}(t)\,\Phi_{mj}(t, \tau)$ and $\Phi_{ij}(t, t) = \delta_{ij}$

$$2D_{ij}(t) = \frac{d\langle X'_{t,i} X'_{t,j}\rangle}{dt} = \int_{t_0}^{t} \Phi_{ik}(t,\tau)\langle V'_k(\tau)V'_j(t)\rangle d\tau + \int_{t_0}^{t} \Phi_{jl}(t,\tau')\langle V'_i(t)V'_l(\tau')\rangle d\tau' + \int_{t_0}^{t}\int_{t_0}^{t} \big[B_{im}(t)\Phi_{mk}(t,\tau)\Phi_{jl}(t,\tau') + B_{jn}(t)\Phi_{ik}(t,\tau)\Phi_{nl}(t,\tau')\big]\langle V'_k(\tau)V'_l(\tau')\rangle d\tau d\tau' \tag{25}$$

where $V'_i(t) = V'_i(\langle\mathbf{X}_t\rangle)$ for simplicity.

[15] If the velocity field is nonstationary but the mean flow is unidirectional, for example, vertical infiltration toward the water table in a stationary porous medium, the only nonzero term in the $\mathbf{B}(t)$ matrix is $B_{11}(t)$, the derivative of longitudinal mean velocity with respect to the longitudinal coordinate. In this case, (19) has the solution $\Phi(t, t_0) = \exp(\int_{t_0}^{t}\mathbf{B}(\tau)d\tau)$, thus (24) reduces to (10)–(14) of *Sun and Zhang* [2000]:

$$X_{ij}(t) = \int_{t_0}^{t}\int_{t_0}^{t} \langle V'_i(\langle\mathbf{X}_\tau\rangle)V'_j(\langle\mathbf{X}_{\tau'}\rangle)\rangle \exp \cdot \left[\int_\tau^t B_{1i}(t')\delta_{i1}dt' + \int_{\tau'}^{t} B_{1j}(t'')\delta_{j1}dt''\right] d\tau d\tau' \tag{26}$$

where the mean velocity direction is aligned with x_1. Note that in (26) the term $\exp\big(\int_\tau^t B_{1i}(t')dt'$ can be explicitly expressed as $\langle V_1(\langle X_t\rangle)\rangle/\langle V_1(\langle X_\tau\rangle)\rangle$. For the case of constant B_{ij}, for example, saturated horizontal flow with constant vertical recharge as studied by *Butera and Tanda* [1999], equation (26) can be further reduced to (26)–(27) of *Butera and Tanda* [1999]. In the special case of $B_{ij} \equiv 0$, i.e., uniform mean velocity field, (19) has the solution $\Phi(t, \tau) \equiv E$ for any t and τ, thus (24) and (25) simplify to

$$\langle X'_{t,i} X'_{t',j}\rangle = \int_{t_0}^{t}\int_{t_0}^{t'} \langle V'_i(\tau)V'_j(\tau')\rangle d\tau d\tau' \tag{27}$$

and

$$2D_{ij}(t) = \int_{t_0}^{t} \langle V'_i(\tau)V'_j(t)\rangle d\tau + \int_{t_0}^{t} \langle V'_i(t)V'_j(\tau')\rangle d\tau'. \tag{28}$$

It should be noted that two integrands in (28) are usually not the same unless the velocity covariance is stationary. In the case that the Lagrangian mean velocity is uniform in some direction i_0, for instance, in the transverse direction of the mean gravity-dominated flow, $\langle V_{i_0}(\langle\mathbf{X}\rangle_t)\rangle = const$, thus $B_{i_0 j}(t) \equiv 0$ for all j and $t \geq 0$, and $\Phi_{i_0 j}(t, \tau) = \delta_{i_0 j}$ for all j and t, $\tau \geq 0$. In this case, the displacement covariance $X_{i_0 i_0}$ and the dispersion coefficient $D_{i_0 i_0}$ in this direction can be calculated using (27) and (28).

[16] Although the first-order particle displacement covariance (27) was originally derived for stationary flow fields

[*Dagan*, 1984, 1989], it has been used for transport in nonstationary flows. For example, *Zhang and Neuman* [1995] employed a similar formula in their study of solute transport in nonstationary flow fields caused by conditioning on measurements; *Rubin and Bellin* [1994] and *Destouni and Graham* [1995] made use of (27) for transport in unidirectional but nonuniform mean flow due to recharge. It is seen from (24) and (26) that when the mean flow is not uniform, a straightforward application of (27) is not appropriate. Instead, (26) should be used if the mean flow is unidirectional as in the cases studied by *Rubin and Bellin* [1994] and *Destouni and Graham* [1995]; (24) should be employed if the flow field is generally nonstationary as in the case of *Zhang and Neuman* [1995]. The goodness of using (27) to approximate (24) or (26) depends on the magnitude of $B_{ij}(t)$. When $B_{ij}(t)$ is negligible, (27) should be able to provide a good approximation for (24) or (26). However, as found by *Sun and Zhang* [2000, Figure 2] in the case of vertical infiltration, excluding the contribution of $B_{11}(t)$ in (26) (i.e., using (27)) induces a significant error when the solute is near the water table where B_{11} is not negligible. Similar results have been obtained by *Butera and Tanda* [1999] for saturated horizontal flow with constant recharge. The significant effect of flow nonstationarity is further verified in one of our examples for a coupled saturated-unsaturated flow. The results from the expression for displacement covariances, i.e., equation (24), are compared against those computed using Dagan's expression, i.e., equation (27). It is shown that our results are in much better agreement with Monte Carlo results than are those from the simpler model.

3. Numerical Implementation

[17] For a given nonstationary saturated-unsaturated porous medium, the first-order Eulerian velocity field and its covariance may be computed using the algorithm developed by *Zhang and Lu* [2002]. For a particle released at location X_0 at time $t = 0$, the first-order Lagrangian velocity field and its covariance can be derived based on the first-order mean Eulerian velocity field and velocity covariances. The mean trajectory is obtained by solving (11), and the derivatives of the first-order Lagrangian velocity field with respect to the mean trajectory (along the particle path), $B_{ij}(t)$, are then calculated.

[18] To compute the second moments $X_{ij}(t) = \langle X'_{t,i}X'_{t,j}\rangle$, one needs to solve for $\Phi(t, \tau)$, where $\tau \le t$ (note that $\Phi(\tau, t) = \Phi^{-1}(t, \tau)$). Because there is no simple analytical expression for $\Phi(t, \tau)$ (unless $\mathbf{B}$ is time-invariant or diagonal, which yields the respective result of $\Phi(t, \tau) = \exp[\mathbf{B}(t - \tau)]$ or $\Phi(t, \tau) = \exp[\int_\tau^t \mathbf{B}(t')dt']$), $\Phi(t, \tau)$ and thus the moment X_{ij} have to be evaluated numerically. Several methods have been proposed for evaluating $\Phi(t, \tau)$ for applications in other fields. One approach is based on (20). This approach, however, is computationally expensive, because a large number of integrations has to be carried out to obtain $\Phi(t, \tau)$ for each pair of t and τ. *Brogan* [1991] proposes an alternative algorithm to estimate $\Phi(t, \tau)$ based on (19). In this study, we adopted and modified Brogan's approach.

1. Set $t_a = \tau$. Let t_δ be a given small time increment. Set $t_b = t_a$.
2. Compute $\phi = \left.\frac{d\Phi(t, t_a)}{dt}\right|_{t=t_b} = \mathbf{B}(t_b)\Phi(t_b, t_a)$.
3. Estimate $\Phi(t_b + t_\delta, t_a) = \Phi(t_b, t_a) + t_\delta\phi$.
4. If $t_b + t_\delta < t$ then let $t_b = t_b + t_\delta$ and repeat steps 2 through 4; if $t_b < t < t_b + t_\delta$, set $t_b = t$ and repeat steps 2 through 4.
5. If $t_b \ge t$, set a new pair of t and τ and start from step 1.

[19] If the Eulerian velocity field changes rapidly in time and/or space, which means that the Lagrangian velocity may change rapidly in time, thus $B_{ij}(t)$ might be relatively large. It may be necessary in this case to change steps 2 and 3 to include the second-order term in the Taylor's expansion of $\Phi(t, \tau)$:

For step 2, compute $\phi = t_\delta\mathbf{B}(t_b)\Phi(t_b, t_a) + \frac{1}{2}t_\delta^2\left[\left.\frac{d\mathbf{B}(t)}{dt}\right|_{t=t_b} + \mathbf{B}^2(t_b)\right]\Phi(t_b, t_a)$.

For step 3, estimate $\Phi(t_b + t_\delta, t_a) = \Phi(t_b, t_a) + \phi$.

[20] The accuracy of the calculated $\Phi(t, \tau)$ value depends on the increment t_δ. Certainly, higher accuracy requires a larger computation effort for each pair of t and τ. However, the number of required pairs of t and τ could be reduced dramatically by using properties of $\Phi(t, \tau)$. Suppose we are going to calculate the covariance $\langle X'_{t,i}X'_{t,j}\rangle$ at time $t_k = t_0 + k\Delta T$, $k = 1, 2, \ldots, K$. The numerical integration involves evaluation of $\Phi(t_k, t_j)$ for $k = 1, 2, \ldots, K$ and $j \le k$. In this case, in fact, we only need to compute $\Phi(t_k, t_{k-1})$, $k = 1, 2, \ldots, K$, using the algorithm described above, because all other terms $\Phi(t_k, t_{k-l})$ for $k = 1, 2, \cdots, K$ and $l = 2, 3, \cdots, k$ can be calculated by utilizing a property of $\Phi(t, \tau)$, i.e., (A3)

$$\Phi(t_k, t_{k-l}) = \Phi(t_k, t_{k-1})\Phi(t_{k-1}, t_{k-l}) = \prod_{i=1}^{l}\Phi(t_{k-i+1}, t_{k-i})$$

$$k = \overline{1, K}; l = \overline{2, k}. \tag{29}$$

Once we have $\Phi(t_k, t_l)$ for all $i = 1, 2, \ldots, K$ and $l = 1, 2, \ldots, k$, the second moments X_{ij} can be calculated using numerical integration. The dispersion coefficient $D_{ij}(t)$ can be evaluated either by using (25) or by taking the derivative of the second moments $X_{ij}(t)$ with respect to t.

4. Illustrative Examples

[21] In this section, we attempt to examine the validity of the developed model to transport of nonreactive solute in hypothetical saturated-unsaturated soils, by comparing model results with those from Monte Carlo simulations. For simplicity, it is assumed in the following examples that the log saturated hydraulic conductivity $f(\mathbf{x}) = lnK_s(\mathbf{x})$ and the pore size distribution parameter α are second-order stationary with an exponential covariance function

$$C_p(\mathbf{h}) = \sigma_p^2\exp(-|\mathbf{h}|/\lambda_p) \tag{30}$$

where $p = f$ or α, σ_p^2 is the variance of p, λ_p is the correlation scale of p, and $\mathbf{h}$ is the separation vector. It is also assumed that f and α are uncorrelated.

[22] We consider a rectangle grid of 20 × 60 square elements in a vertical cross-section having a width $L_2 = 120$ cm and a height $L_1 = 360$ cm. Thus the size of each element is 6.0 cm by 6.0 cm. The input parameters are given as $\langle f\rangle = 0.0$ (i.e., the geometric mean of the saturated hydraulic conductivity $K_G = 1.0$ cm/T), $\sigma_f^2 = 0.2$, $\langle\alpha\rangle = 0.05$ cm^{-1}, $\sigma_\alpha^2 = 1.0 \times 10^{-4}$ cm^{-2}, $\lambda_f = \lambda_\alpha = 30$ cm, $\theta_s = 0.3$, $\theta_r = 0.0$, and an infiltration rate of $Q = -0.04$ cm/T (where T is any time unit, as long as it is consistent with the time unit in

K_G). In terms of coefficients of variation, the variabilities of K_s and α are $CV_{Ks} = \sigma_{Ks}/\langle K_s \rangle = 44.7\%$ and $CV_\alpha = \sigma_\alpha/\langle \alpha \rangle = 20.0\%$, respectively.

[23] We design three cases to test our model. For each case, we conduct Monte Carlo simulations and compare results against those from our stochastic model. We first generate 10,000 two-dimensional 20 $\times$ 60 unconditional Gaussian realizations with a zero mean, a unit variance, and a correlation length $\lambda = 30$ cm, using a sequential Gaussian random field generator *sgsim* from GSLIB [*Deutsch and Journel*, 1998]. The quality of these Gaussian random fields is checked first by comparing the sample mean and variance of these unconditional realizations with the specified zero mean and unit variance. The sample variogram calculated from generated realizations is then compared with the analytical exponential model (30). These comparisons indicate that the generated Gaussian realizations reproduce the specified mean, variance, and correlation length very well. These zero mean, unit variance realizations are then scaled to obtain realizations with the specified means and variances for f and α.

[24] For each simulation (with one realization for f and α each), a nonreactive particle is placed at a given point in the flow domain. If the flow solution for this simulation converges, the position of the particle at any given time can be determined from the Lagrangian velocity field, which is converted from the Eulerian velocity field. We record the particle's position at some given times until the particle leaves the domain. If the flow solution does not converge due to the variations in the f and α fields, the simulation is ignored and the two particular realizations of f and α for this simulation are skipped. Excluding some realizations may change the degree of heterogeneity and the spatial structure of the f and α fields because those discarded are most likely the realizations with large contrasts in f and α fields [*Zhang and Lu*, 2002]. In turn, there may exist a discrepancy between the flow moments from the Monte Carlo simulations and the stochastic flow moment approach of *Zhang and Lu* [2002]. In our examples, we use the sample mean velocity field and sample velocity covariances calculated from Monte Carlo simulations as the input Eulerian mean velocity field and velocity covariances to the first-order stochastic transport model. We do so to ensure that the stochastic transport model and the Monte Carlo transport simulations have the same underlying flow field and are thus compatible. Therefore the causes for any difference between the two sets of results would be the truncation errors in neglecting higher-order terms in the first-order stochastic transport model, the numerical errors associated with approximating the first-order expressions and with particle tracking in the Monte Carlo simulations, and the statistical sampling errors occurred in the Monte Carlo simulations.

[25] The particle's mean position and spreading at any given time are then calculated using particle's positions at that time from all Monte Carlo simulations. Because the particle may leave the flow domain earlier in some Monte Carlo simulations than in others, we calculate the particle's mean position and spreading only up to the maximum time at which the particle remains within the flow domain for all simulations.

[26] In our first example, denoted as case 1, we consider solute transport in a mean gravity-dominated flow. The boundary conditions are specified as follows: no-flow at two vertical boundaries ($x_2 = 0.0$ and $x_2 = 120$ cm), a constant deterministic flux $Q = -0.04$ cm/T (a negative value means infiltration) at the top ($x_1 = 360$ cm), constant pressure head $\psi_0 = -61.915$ cm at the bottom, where ψ_0 is determined from the infiltration rate Q and the specified $\langle f \rangle$, σ_f^2, and $\langle \alpha \rangle$ using the formula $Q = -K = -\exp(\langle f \rangle + \sigma_f^2/2) \exp(\langle \alpha \rangle \psi_0)$.

[27] In the second example (case 2), the boundary conditions are similar to those in case 1, except that the bottom is the water table ($\psi_0 = 0.0$). The third example (case 3) is solute transport in a coupled unsaturated-saturated flow system. The boundary conditions are given as: no-flow at the bottom ($x_1 = 0.0$), a constant deterministic flux $Q = -0.04$ cm/T at the top ($x_1 = 360$ cm), constant total heads $H = 60$ cm and $H = 54$ cm at the lower portion ($x_1 \leq 60$ cm) of the left side and the lower portion ($x_1 \leq 54$ cm) of the right side, respectively, and no-flow at the upper portion of the left and right sides. Under the given conditions, the upper portion of the flow domain is unsaturated while the lower portion is saturated with a horizontal flow from the left to the right. All boundary conditions for three cases are deterministic.

5. Results and Discussions

5.1. Nonstationarity of Velocity Fields

[28] Monte Carlo simulations have been conducted for each case. The mean flow for these cases derived from Monte Carlo simulations are depicted in Figure 1, where the arrowed curves stand for streamlines, the solid curves represent contours for the vertical component of the mean velocity, and the dotted ones are contours for the horizontal component of the mean velocity. A particle is released at ($x_1 = 350$ cm and $x_2 = 60$ cm) in cases 1 and 2, while it is released at ($x_1 = 350$ cm and $x_2 = 30$ cm) in case 3. The circles on streamlines stand for the mean position of the particle at different times (40 T between two adjacent circles).

[29] For the mean gravity-dominated flow (Figure 1a) because the mean pressure head ψ is constant (=-61.915 cm) over the entire domain and the f and α fields are by assumption statistically homogeneous, the effective moisture content and thus the mean velocity are constant. The particle moves downward at a constant rate. In the case of the water table boundary at the bottom (case 2), though the mean flux is the same over the entire flow domain, the mean velocity is a function of depth, due to the fact that close to the water table the effective moisture content increases. Toward the water table, the distance between two adjacent circles becomes smaller (Figure 1b), which implies that the particle is decelerated.

[30] For the case of flow in a saturated-unsaturated porous medium (case 3), in the upper portion of the domain the mean velocity is a constant and the flow is downward driven by gravity. Near the water table, the flow changes its direction and tends to merge into the flow in the saturated zone. Similar to that in case 2, toward the water table, the particle decelerated but it accelerates after it crosses the water table due to a large horizontal flux component in the saturated zone.

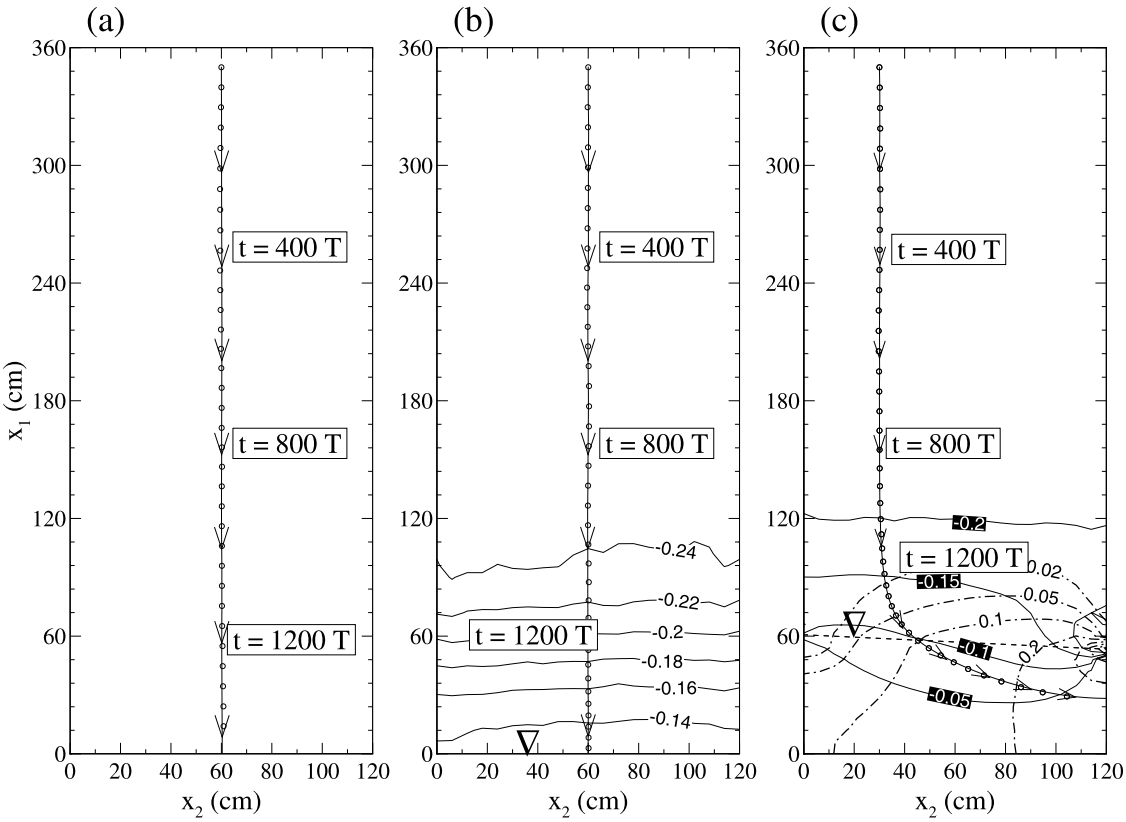

Figure 1. Mean flow and streamlines for three cases: (a) mean gravity-dominated flow (case 1); (b) a water table at the bottom (case 2); (c) unsaturated-saturated flow (case 3).

[31] The particle positions at some elapsed times are shown in Figure 2, where points with different colors represent different elapsed times, and each point stands for the particle position at a particular elapsed time in a single realization of the Monte Carlo simulations. Some observations may be made from the particle plumes. At the early time of $t = 100\ T$, the plumes are almost the same for the three cases; at $t = 500\ T$, the plumes for cases 1 and 2 are similar while the plume for case 3 is narrower in the horizontal direction. At $t = 1000\ T$, the plume for case 1 is somewhat wider than that for case 2 in both directions, and the plume for case 3 lags behind the other two plumes and is significantly narrower. At $t = 1500\ T$, parts of the plumes for cases 1 and 2 have reached and exit the bottom boundaries; the plume for case 3 passes the water table into the saturated zone, changes its direction, and becomes highly distorted. After the plume passes the water table it becomes mainly horizontal.

[32] The sample Eulerian mean velocity field and sample velocity covariances calculated from Monte Carlo simulations are converted, based on the position at which the particle is released, to the Lagrangian mean velocity field and the corresponding velocity covariances, which are used in our stochastic model. It should be pointed out that though both f and α are assumed to be stationary, the velocity covariance is nonstationary in all these cases. Figure 3 illustrates covariances of the Lagrangian velocity fields for the cases. For each case the longitudinal and transverse Lagrangian velocity covariances $C_{u_1u_1}$ and $C_{u_2u_2}$ with respect to two reference points (times), one being t_0 at which the particle is released and the other being t_n, which is the maximum time before the particle exits the flow domain, are plotted against the separation time lag (or separation distance). In the case of the mean gravity-dominated flow, if the domain is unbounded and the field is stationary, the longitudinal velocity covariance should be stationary with an exponential model having a finite integral scale, and the transverse velocity covariance should follow a hole-type function with a zero integral scale [*Russo*, 1993].

[33] However, the presence of boundaries causes the velocity covariances to be nonstationary in that the velocity covariance between any two points depends on actual locations of these points rather than only their space or time lags. Figure 3a shows that there is a big difference between the covariances $C_{u_1u_1}$ with respect to the two reference points. Because the reference point t_n corresponds to a location close to the bottom boundary, the transverse velocity covariance $C_{u_2u_2}(t_n, t_i)$ is close to zero, owing to the specific boundary condition at the bottom. For the case with the water table at the bottom (Figure 3b) the velocity covariance $C_{u_1u_1}$ with respect to the reference time t_0, which corresponds to the starting point (350, 60), is close to an exponential model, while the corresponding $C_{u_2u_2}$ appears to be a hole-type function. Again, the velocity covariances are not stationary as the velocity covariances with respect to t_n are significantly different from their counterparts at t_0. Because the velocity covariance plays an important role in calculation of the displacement covariance X_{ij}, the existing stochastic transport models based on the assumption of stationary velocity covariances may not be adequate for simulating solute transport in the unsaturated zone. For case 3 of the coupled unsaturated-saturated flow, the velocity

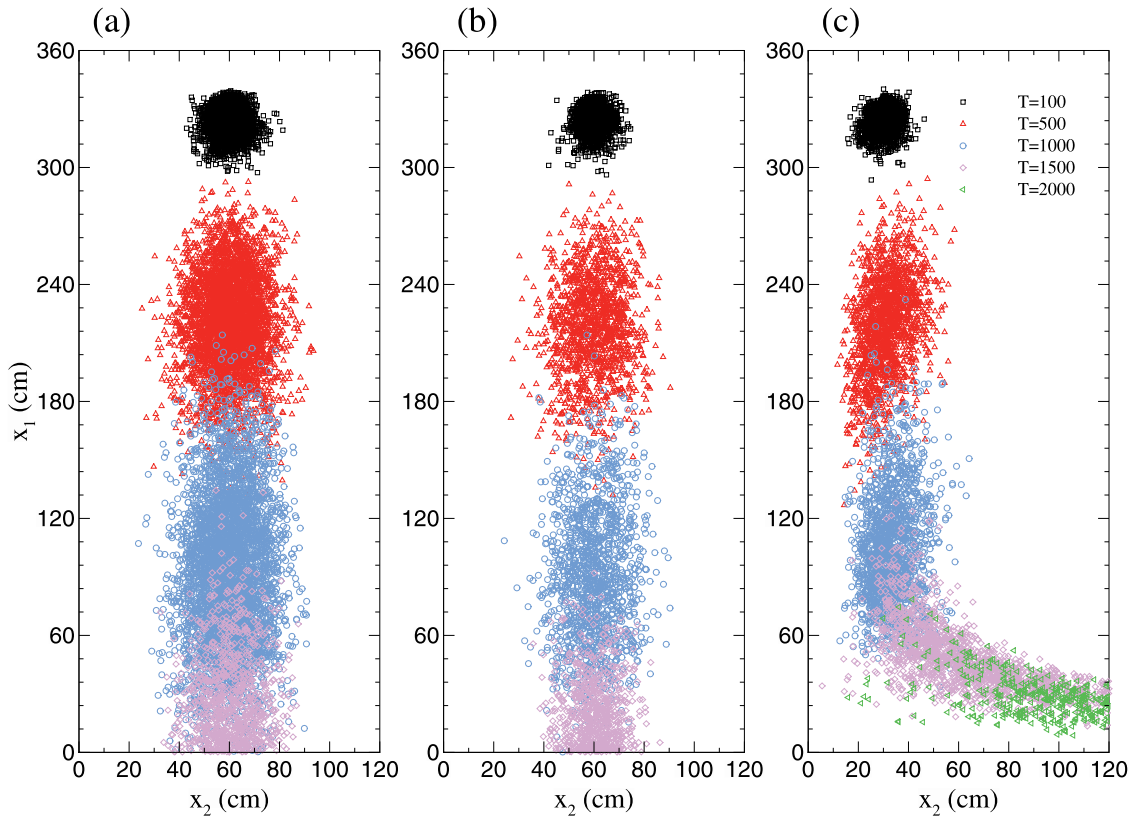

Figure 2. Particle positions at different elapsed times obtained from Monte Carlo simulations: (a) case 1; (b) case 2; (c) case 3.

covariances are even more location dependent. The reference time t_0 corresponds to a point in the mean gravity-dominated unsaturated flow regime, where the flow is predominantly vertical, whereas the reference time t_n corresponds to a point near the right-hand side boundary in the saturated zone, where the mean flow is mainly horizontal. Hence, the velocity covariance components $C_{u_1u_1}$ and $C_{u_2u_2}$ switch their roles at the two times (Figure 3c). Between these two times, the mean flow, and thus the mean particle path line, changes direction, especially near the interface of the two flow regimes.

5.2. Statistical Moments of Particles

[34] Comparisons between the particle moments from the stochastic model and the Monte Carlo simulations are illustrated in Figures 4–6, where the Figures 4a, 5a, and 6a are for comparison of the mean position, and Figures 4b, 5b, and 6b for comparison of displacement covariance. The curves for Monte Carlo simulation results are shorter than those for our stochastic modeling results because for the former, once the particle in one simulation leaves the flow domain at a certain time, we are not able to compute the sample mean position and displacement covariance thereafter. Figures 4–6 indicate that there is an excellent agreement between Monte Carlo simulation results and the first-order stochastic transport model results for the cases of given f and α variabilities and specific flow configurations. It is expected that the agreement between the two approaches should deteriorate as the level of variabilities increases. Although the examples shown in this study do not reveal the validity range of the first-order stochastic transport model, they serve the purpose to demonstrate that the first-order transport model correctly captures the effects of flow nonstationarity on solute spreading.

[35] It is interesting to see the behavior of the mean trajectory and the displacement covariances X_{11} and X_{22} over time for different flow scenarios. Figure 4a shows changes of the mean particle position over time for the mean gravity-dominated flow. Linear vertical and constant horizontal components of the mean trajectory indicate that the particle moves downward at a constant rate. The spreading in the longitudinal (vertical) direction, X_{11}, is always increasing over time (Figure 4b), while in the transverse (horizontal) direction, the spreading increases at the early time and remains more or less constant, except at late times when the boundary effects become effective.

[36] As mentioned before, the flow of this case would be stationary if it was without boundary effects. Under the condition of stationary, mean gravity-dominated flow, the particle displacement covariances have been well studied [e.g., *Russo*, 1993, 1995a, 1995b, 1998; *Harter and Zhang*, 1999]. For the case with the water table at the bottom, a constant $\langle X_2 \rangle$ means that the particle moves downward (Figure 5a). At the early time, the plot of $\langle X_1 \rangle$ over time is a straight line, similar to the case of the mean gravity-dominated flow. When the particle approaches the water table, the slope of the $\langle X_1 \rangle$ curve decreases, indicating that near the water table the particle decelerates, which causes the displacement covariance X_{11} to decrease at the late time (Figure 5b). It should be noted that both X_{11} and X_{22} decrease at the late time, that is, near the water table, the distribution of particles shrinks in both longitudinal

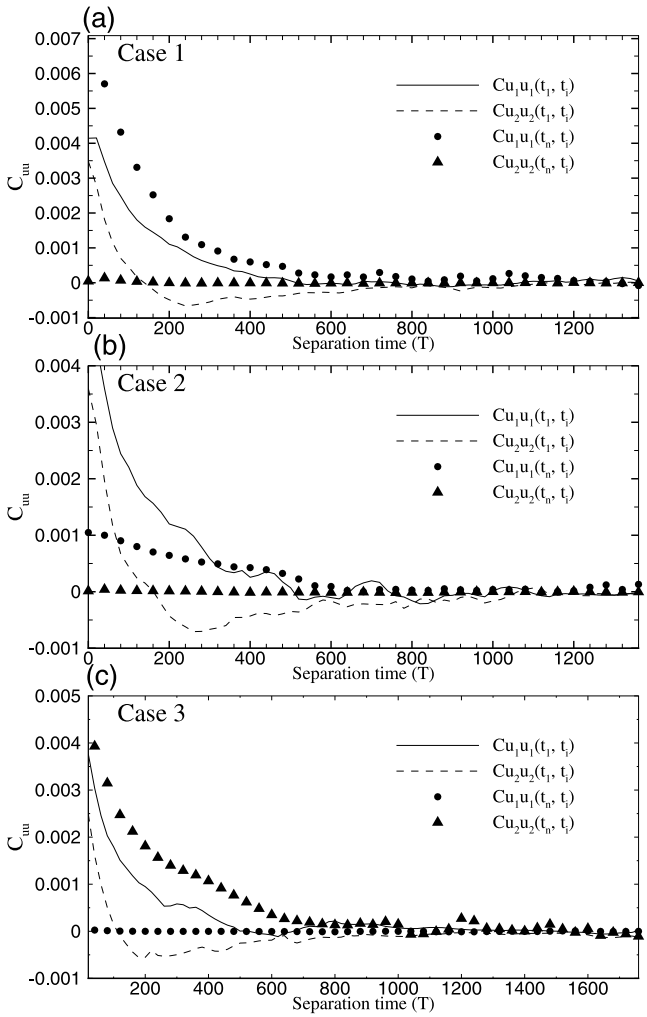

Figure 3. Lagrangian velocity covariances between points along the mean particle path and two reference points, one at which the particle is released and the other at which the particle exits the domain, for all three cases.

and transverse directions (also see Figure 2b). The decrease in X_{11} near the water table has been observed by *Sun and Zhang* [2000] for transport in unidimensional flow. The finding is also consistent with the observation of *Russo* [1993] for the mean gravity-dominated flow that both longitudinal and transverse displacement covariance decrease as the water saturation increases. The time at which both X_{11} and X_{22} start to decrease depends on soil properties. In general, if the pore size parameter α is large, the mean gravity-dominated regime will be longer, and the impact of the water table boundary on X_{ii} will be smaller.

[37] For the case of flow in a saturated-unsaturated porous medium (case 3), at early times ($t \leq 800\ T$) the plot of $\langle X_1(t) \rangle$ is a straight line and the displacement covariances X_{11} and X_{22} increase with time, which indicates that the mean flow is gravity driven in the upper portion of the domain. Thereafter, the decrease in the slope of the $\langle X_1 \rangle$ curve again corresponds to the decrease of the vertical (Eulerian) velocity component near the water table (Figure 6a). After the particle crosses the water table, it moves much faster in the horizontal direction than in the vertical direction (Figure 6a). The horizontal particle displacement covariance increases rapidly while the vertical counterpart decreases.

[38] The effect of flow nonstationarity on displacement covariances for the case with a water table boundary has been studied by *Sun and Zhang* [2000]. For the coupled saturated-unsaturated flow, the effect of flow nonstationarity is also significant, as shown in Figure 6b, where displacement covariances resulted from our model, i.e., equation (24), are compared with both Monte Carlo results and those from Dagan's expression, i.e, equation (27). Figure 6b shows that results from our model are in much better agreement with Monte Carlo results than are those obtained by ignoring the effect of flow nonstationarity, i.e, Dagan's expression. More specifically, for a particle initiated in the unsaturated zone, displacement covariance X_{11} increases with time, and as the particle approaches to the water table X_{11} starts to decrease, as predicted by our model and verified by Monte Carlo simulation, while it

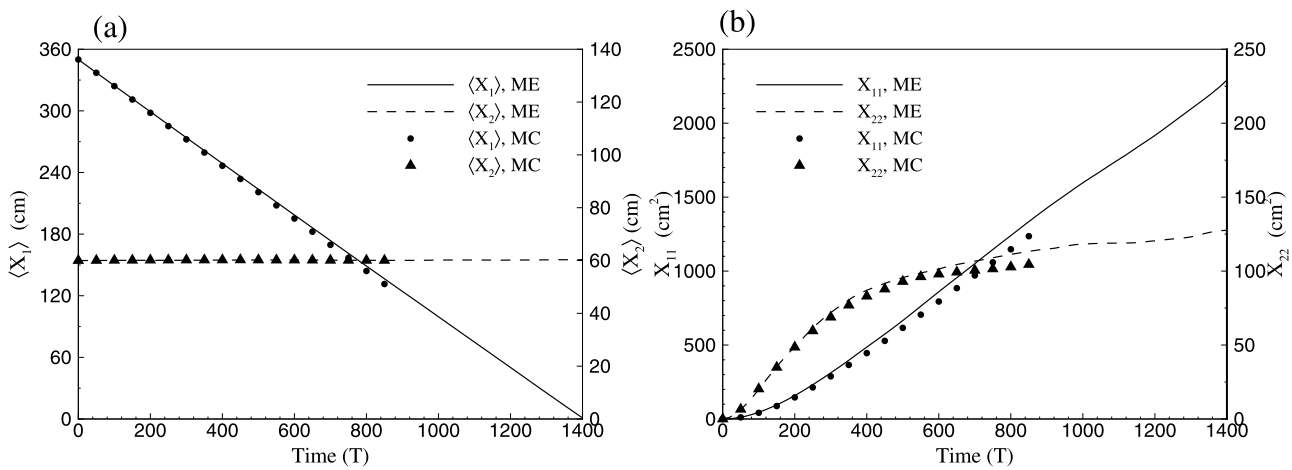

Figure 4. Comparison of the mean position and displacement covariances between Monte Carlo results (MC) and first-order stochastic model results (ME) for the mean gravity-dominated flow.

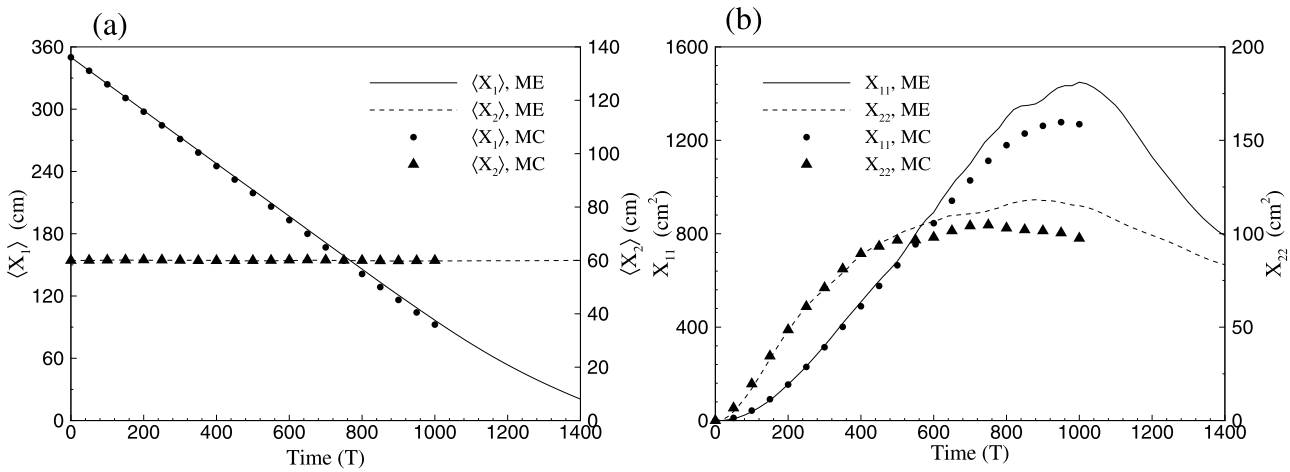

Figure 5. Comparison of the mean position and displacement covariances between Monte Carlo results (MC) and first-order stochastic model results (ME) for the case with a water table at the bottom.

will continue to increase if the effect of flow nonstationarity is ignored. After passing through the water table, the displacement covariance X_{22} increases quickly in both our model and Monte Carlo simulation, while such increase is delayed if the effect of nonstationarity in mean flow is ignored.

[39] The mixed term of the displacement covariance tensor, X_{12}, for all three cases is illustrated in Figure 7. Figure 7 shows that for each case X_{12} calculated from Monte Carlo simulations and that from our model are in good agreement. In addition, for cases 1 and 2, comparing to their corresponding longitudinal displacement covariance X_{11}, the mixed term X_{12} is very small due to limited transverse flux in both cases. Small X_{12} also implies that the solute plume moves unidirectionally and does not have a significant rotation. However, for case 3, both Monte Carlo results and our model results show that $X_{12}(t)$ is relatively large, which indicates a significant plume rotation and distortion. It should be noted that when the plume is highly distorted (near the water table), the first two particle moments (mean positions and displacement covariances) are not enough to adequately describe the state of the plume.

5.3. Macrodispersion

[40] The macrodispersion coefficients D_{11} and D_{22} are illustrated in Figures 8a and 8b, respectively. Figure 8a shows that for the mean gravity-dominated flow, D_{11} increases at the early time and then remains almost constant. For cases 2 and 3, because of the effect of the water table, D_{11} starts to decrease from about $t = 600\ T$ indicating that X_{11} increases at a slower rate. D_{11} decreases further to negative values of D_{11}, which correspond to the decrease of the displacement covariance X_{11}. At late time D_{11} increases toward zero (but still being negative), indicating that the rate of decrease of X_{11} becomes smaller.

[41] In the transverse direction in case 2, because $\langle V_2(\langle \mathbf{X}_t \rangle)\rangle \equiv 0$, D_{22} can be calculated using (28):

$$D_{22} = \int_{t_0}^{t} \langle V_2'(\tau) V_2'(t)\rangle d\tau. \tag{31}$$

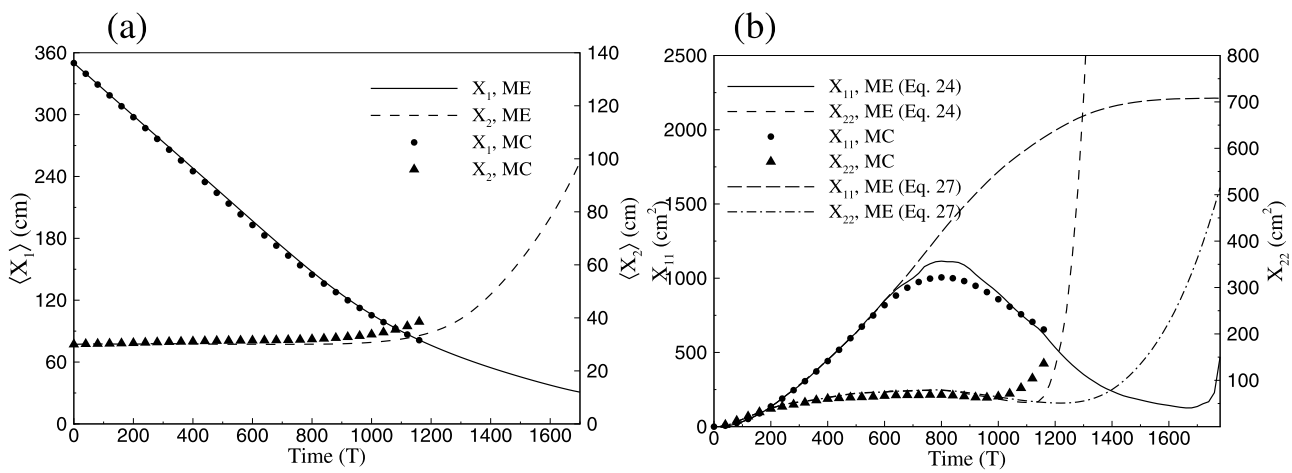

Figure 6. Comparison of (a) the mean position between Monte Carlo results (MC) and first-order stochastic model results (ME) and (b) displacement covariances between MC, ME using equation (24) and ME using Dagan's expression, i.e., equation (27), for the saturated-unsaturated flow.

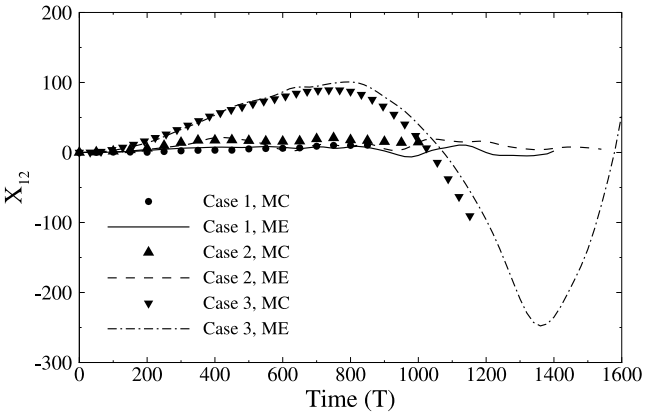

Figure 7. Mixed displacement covariances X_{12} for three cases.

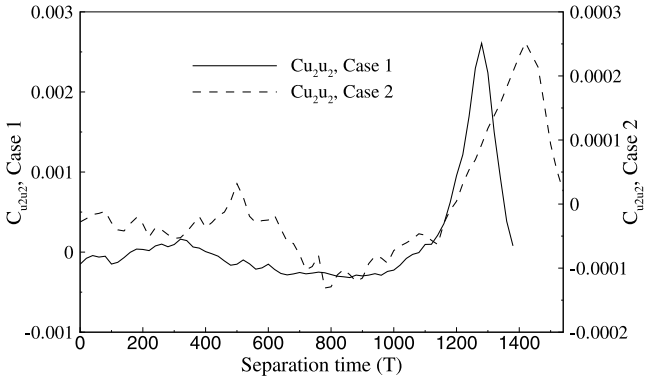

Figure 9. Transverse Lagrangian velocity covariances between points along the mean particle path and a reference point close to the bottom boundary for cases 1 and 2.

To explore the behavior of X_{22} near the water table boundary, we consider an elapsed time t_p = 1450 T which is 100 T before the mean particle position reaches the boundary. The transverse Lagrangian velocity covariance $C_{u_2u_2}(t, t_p)$ is shown as the dashed curve in Figure 9. The dispersion coefficient $D_{22}(t_p)$ in fact is the integration of the dashed curve from initial time t = 0.0 to $t = t_p$ (the highest peak on the dashed curve). It is obvious that D_{22} is negative, which means that X_{22} is decreasing near the water table boundary. In contrast, for the case of mean gravity-dominated flow, the dispersion coefficient $D_{22}(t_p)$, which is the integration of the solid curve in Figure 9 from t = 0 to t_p (the highest peak on the solid curve), is positive. That is, for mean gravity-dominated flow X_{22} is still increasing near the boundary.

[42] It is noteworthy that for both cases 1 and 2, D_{22} = 0 at the lower boundary. This could be easily explained if we realize that the transverse velocity variance at the lower boundary is zero. In fact, at the lower boundary, since the deterministic total head is the same along the boundary, the transverse velocity perturbation $V_2' \equiv 0$; thus the variance of the transverse velocity on the lower boundary is zero and so is the transverse velocity covariance between any boundary point t_p and points on the particle path therefore from (31) $D_{22}(t_p)$ = 0. This implies that at the lower boundary the decreasing X_{22} reaches its minimum for case 2 and that the increasing X_{22} reaches its maximum for case 1.

6. Summary and Conclusions

[43] In this paper, we presented a general approach to predict spreading of nonreactive solute in transient nonstationary flows in bounded, heterogeneous unsaturated-saturated media. The Eulerian transient mean velocity and velocity covariance may be obtained using the algorithm developed by *Zhang and Lu* [2002] and converted to Lagrangian mean velocity and covariance. Using a first-order approximation, the moments of the particle trajectory are related to the Lagrangian velocity field. We derived an expression for the displacement covariance tensor $X_{ij}(t)$ in terms of the initial displacement covariance at $t = t_0$, the Lagrangian velocity covariance at the mean position $\langle \mathbf{X}_t \rangle$, and the state transition matrix $\Phi(t, \tau)$, the last of which is the derivative of the Lagrangian mean velocity at $\langle \mathbf{X}_t \rangle$ with respect to the particle path. In the case that the flow field is stationary and unidirectional, the state transition matrix $\Phi(t, \tau)$ equals the identical matrix and our expression reduced to the well-known expression of *Dagan* [1984]. For the nonstationary but unidirectional flow, $\Phi(t, \tau)$ is an exponential matrix function and our expression reduced to

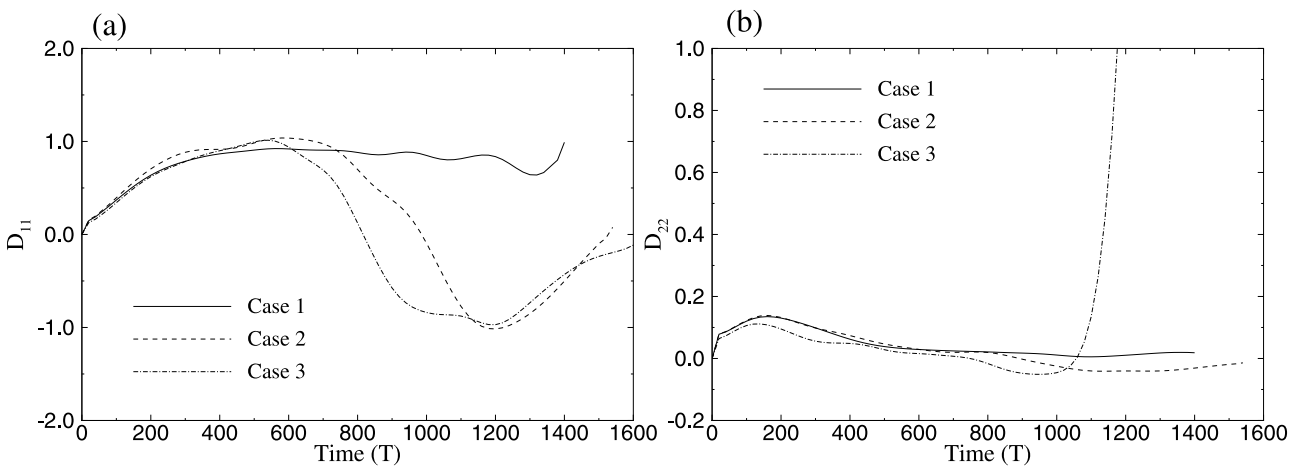

Figure 8. Macrodispersion coefficients D_{11} and D_{22} for three cases.

those of *Butera and Tanda* [1999] and *Sun and Zhang* [2000]. In general, $\Phi(t, \tau)$ has to be solved numerically. The mean trajectory and displacement covariance are then evaluated through numerical integrations. The macrodispersion coefficient D_{ij} can also be evaluated numerically.

[44] The stochastic Lagrangian transport model developed in the current study is in spirit similar to that of *Indelman and Rubin* [1996] in the way of handling the effects of mean flow nonuniformity on solute transport. However, our work presents an improvement over the latter in the following aspects: (1) Indelman and Rubin's main result [*Indelman and Rubin*, 1996, equation (16)] seems to be only valid for weak mean flow nonuniformity while our model does not have this restriction; (2) our study investigated transport in coupled unsaturated and saturated flow where the mean flow direction and magnitude may vary significantly in space, while they only evaluated the special case of unidirectional mean flow. Our work is different from other previous studies on transport in nonuniform flows [*Butera and Tanda*, 1999; *Sun and Zhang*, 2000; *Destouni et al.*, 2001] in that the latter are all concerned with the special case of unidirectional mean flows.

[45] We designed three cases to examine the validity of the first-order stochastic transport model. Monte Carlo simulations have been conducted for all cases, and the sample velocity fields from Monte Carlo simulations are used as input to the transport model. It is shown that the model results are in good agreement with those of Monte Carlo simulations. The validity of the transport model was also verified by comparing its results with those from the existing models for the cases of mean gravity-dominated flow and the saturated flow with a water table boundary.

Appendix A

[46] Consider the homogeneous system of (17):

$$\frac{d\mathbf{X}'_t}{dt} = \mathbf{B}(t)\mathbf{X}'_t \tag{A1}$$

with initial data $\mathbf{X}'_t = \mathbf{X}'_{t_0}$. The fundamental matrix (or state transition matrix) $\Phi(t, t_0)$ corresponding to (A1) satisfies

$$\frac{d\Phi(t, t_0)}{dt} = \mathbf{B}(t)\Phi(t, t_0) \tag{A2}$$

with initial condition $\Phi(t_0, t_0) = E$, the identity matrix. The state transition matrix has several important properties including

$$\Phi(t_2, t_0) = \Phi(t_2, t_1)\Phi(t_1, t_0) \tag{A3}$$

and

$$[\Phi(t_1, t_0)]^{-1} = \Phi(t_0, t_1). \tag{A4}$$

The transition matrix can be thought of as a map which takes the initial data to the solution of (A1):

$$\mathbf{X}'_t = \Phi(t, t_0)\mathbf{X}'_{t_0}. \tag{A5}$$

For the original equation (17), assuming that its solution can be written as

$$\mathbf{X}'_t = \Phi(t, t_0)c(t), \tag{A6}$$

substituting (A6) into (17) and using (A2), one obtains

$$\frac{dc(t)}{dt} = [\Phi(t, t_0)]^{-1}\mathbf{V}'(\langle \mathbf{X}_t \rangle), \tag{A7}$$

which has the solution

$$c(t) = c(t_0) + \int_{t_0}^{t} \Phi(t_0, \tau)\mathbf{V}'(\langle \mathbf{X}_\tau \rangle)d\tau. \tag{A8}$$

Because $c(t_0) = \mathbf{X}'_{t_0}$, substituting (A8) into (A6) immediately leads to (18):

$$\mathbf{X}'_t = \Phi(t, t_0)\mathbf{X}'_0 + \int_{t_0}^{t} \Phi(t, \tau)\mathbf{V}'(\langle \mathbf{X}_\tau \rangle)d\tau. \tag{A9}$$

References

Antsaklis, P. J., and A. N. Michel, *Linear Systems*, McGraw-Hill, New York, 1997.

Bresler, E., and G. Dagan, Convective and pore scale dispersive solute transport in unsaturated heterogeneous fields, *Water Resour. Res.*, *17*, 1683–1693, 1981.

Brogan, W. L., *Modern Control Theory*, 3rd ed., Prentice-Hall, Old Tappan, N. J., 1991.

Butera, I., and M. G. Tanda, Solute transport analysis through heterogeneous media in nonuniform in the average flow by a stochastic approach, *Transp. Porous Media*, *36*, 255–291, 1999.

Cushman, J. H., and T. R. Ginn, Nonlocal dispersion in media with continuous evolving scales of heterogeneity, *Transp. Porous Media*, *13*, 123–138, 1993.

Dagan, G., Solute transport in heterogeneous porous formations, *J. Fluid Mech.*, *145*, 151–177, 1984.

Dagan, G., *Flow and Transport in Porous Formations*, Springer-Verlag, New York, 1989.

Dagan, G., and E. Bresler, Solute dispersion in unsaturated heterogeneous soil at field scale: Theory, *Soil Sci. Soc. Am. J.*, *43*, 461–467, 1979.

Destouni, G., and W. D. Graham, Solute transport through an integrated heterogeneous soil-groundwater system, *Water Resour. Res.*, *31*, 1935–1944, 1995.

Destouni, G., E. Simic, and W. D. Graham, On the applicability of analytical methods for estimating solute travel time statistics in nonuniform groundwater flow, *Water Resour. Res.*, *37*, 2303–2308, 2001.

Deutsch, C. V., and A. G. Journel, *GSLIB: Geostatistical Software Library*, 340 pp., Oxford Univ. Press, New York, 1998.

Foussereau, X., W. D. Graham, G. A. Akpoji, G. Destouni, and P. S. C. Rao, Solute transport through a heterogeneous coupled vadose-saturated zone system with temporally random rainfall, *Water Resour. Res.*, *37*, 1577–1588, 2001.

Gardner, W. R., Some steady-state solutions of the unsaturated moisture flow equation with application to evaporation from a water table, *Soil Sci.*, *85*, 228–232, 1958.

Gelhar, L. W., and C. L. Axness, Three-dimensional stochastic analysis of macrodispersion in aquifers, *Water Resour. Res.*, *19*(1), 161–180, 1983.

Graham, W., and D. McLaughlin, Stochastic analysis of nonstationary subsurface solute transport, 2, Conditional moments, *Water Resour. Res.*, *25*(11), 2331–2355, 1989.

Harter, T., and T.-C. J. Yeh, Stochastic analysis of solute transport in heterogeneous, variably saturated soils, *Water Resour. Res.*, *32*, 1585–1595, 1996a.

Harter, T., and T.-C. J. Yeh, Conditional stochastic analysis of solute transport in heterogeneous, variably saturated soils, *Water Resour. Res.*, *32*, 1597–1609, 1996b.

Harter, T., and D. Zhang, Water flow and solute spreading in heterogeneous soils with spatially variable water content, *Water Resour. Res.*, *35*, 415–426, 1999.

Indelman, P., and Y. Rubin, Solute transport in nonstationary velocity fields, *Water Resour. Res.*, *32*, 1259–1267, 1996.

Jury, W. A., Simulation of solute transport using a transfer function model, *Water Resour. Res.*, *18*, 363–368, 1982.

Jury, W. A., and D. R. Scotter, A unified approach to stochastic convective transport problems, *Soil Sci. Soc. Am. J.*, *58*, 1327–1336, 1994.

Jury, W. A., G. Sposito, and R. E. White, A transfer function model of solute transport through soil, 1, Fundamental concepts, *Water Resour. Res.*, *22*, 243–247, 1986.

Kavvas, M. L., and A. Karakas, On the stochastic theory of solute transport by unsteady and steady groundwater flow in heterogeneous aquifers, *J. Hydrol.*, *179*, 321–351, 1996.

Lu, Z., and D. Zhang, Stochastic analysis of transient flow in heterogeneous, variably saturated porous media: The van Genuchten-Mualem constitutive model, *Vadose Zone J.*, *1*, 137–149, 2002.

Neuman, S. P., C. L. Winter, and C. M. Newman, Stochastic theory of field-scale Fickian dispersion in anisotropic porous media, *Water Resour. Res.*, *23*, 453–466, 1987.

Polmann, D. J., D. McLaughlin, S. Luis, L. W. Gelhar, and R. Ababou, Stochastic modeling of large-scale flow in heterogeneous unsaturated soils, *Water Resour. Res.*, *27*, 1447–1457, 1991.

Rubin, Y., Stochastic modeling of macrodispersion in heterogeneous media, *Water Resour. Res.*, *26*, 133–142, 1990.

Rubin, Y., Transport of inert solutes by groundwater: Recent developments and current issues, in *Subsurface Flow and Transport: A Stochastic Approach*, edited by G. Dagan and S. P. Neuman, pp. 115–132, Cambridge Univ. Press, New York, 1997.

Rubin, Y., and A. Bellin, The effects of recharge on flow nonuniformity and macrodispersion, *Water Resour. Res.*, *30*, 939–948, 1994.

Russo, D., Determining soil hydraulic properties by parameter estimation: On the selection of a model for the hydraulic properties, *Water Resour. Res.*, *24*, 453–459, 1988.

Russo, D., Stochastic modeling of macrodispersion for solute transport in a heterogeneous unsaturated porous formation, *Water Resour. Res.*, *29*, 383–397, 1993.

Russo, D., On the velocity covariance and transport modeling in heterogeneous anisotropic porous formations, 2, Unsaturated flow, *Water Resour. Res.*, *31*, 139–145, 1995a.

Russo, D., Stochastic analysis of the velocity covariance and the displacement covariance tensors in partially saturated heterogeneous anisotropic porous formations, *Water Resour. Res.*, *31*, 1647–1658, 1995b.

Russo, D., Stochastic analysis of flow and transport in unsaturated heterogeneous porous formation: Effects of variability in water saturation, *Water Resour. Res.*, *34*, 569–581, 1998.

Russo, D., and M. Bouton, Statistical analysis of spatial variability in unsaturated flow parameters, *Water Resour. Res.*, *28*, 1925–1991, 1992.

Shvidler, M. I., Correlation model of transport in random fields, *Water Resour. Res.*, *29*, 3189–3199, 1993.

Simmons, C. S., A stochastic convective transport representative of dispersion in one-dimensional porous media systems, *Water Resour. Res.*, *18*, 1193–1214, 1982.

Sun, A. Y., and D. Zhang, Prediction of solute spreading during vertical infiltration in unsaturated, bounded heterogeneous media, *Water Resour. Res.*, *36*, 715–723, 2000.

van Genuchten, M. T., A closed-form equation for predicting the hydraulic conductivity of unsaturated soils, *Soil Sci. Soc. Am. J.*, *44*, 892–898, 1980.

Winter, C. L., C. M. Newman, and S. P. Neuman, A perturbation expansion for diffusion in a random velocity field, *SIAM J. Appl. Math.*, *44*(2), 411–424, 1984.

Yeh, T.-C. J., W. Gelhar, and A. L. Gutjahr, Stochastic analysis of unsaturated flow in heterogeneous soils, 1, Statistically isotropic media, *Water Resour. Res.*, *21*, 447–456, 1985a.

Yeh, T.-C. J., W. Gelhar, and A. L. Gutjahr, Stochastic analysis of unsaturated flow in heterogeneous soils, 2, Statistically anisotropic media with variable α, *Water Resour. Res.*, *21*, 457–464, 1985b.

Zhang, D., *Stochastic Methods for Flow in Porous Media: Coping with Uncertainties*, Academic, San Diego, Calif., 2002.

Zhang, D., and Z. Lu, Stochastic analysis of flow in a heterogeneous unsaturated-saturated system, *Water Resour. Res.*, *38*(2), 1018, doi:10.1029/2001WR000515, 2002.

Zhang, D., and S. P. Neuman, Eulerian-Lagrangian analysis of transport conditioned on hydraulic data, 1, Analytical-numerical approach, *Water Resour. Res.*, *31*, 39–51, 1995.

Zhang, D., T. C. Wallstrom, and C. L. Winter, Stochastic analysis of steady-state unsaturated flow in heterogeneous media: Comparison of the Brooks-Corey and Gardner-Russo models, *Water Resour. Res.*, *34*, 1437–1449, 1998.

Z. Lu and D. Zhang, Hydrology, Geochemistry, and Geology Group (EES-6), Los Alamos National Laboratory, MS T003, Los Alamos, NM 87545, USA. (zhiming@lanl.gov)